

Radio Occultation and Heavy Precipitation with PAZ (ROHP-PAZ)

Data User Guide

Reference	ROHP-PAZ_DUG_v1
Version:	1.0
Prepared by:	E.Cardellach, R. Padullés, S. Oliveras
Reviewed by:	E. Cardellach
Date:	April 16, 2020

1. RO in PAZ: Brief Summary	2
1.1 Lower Level Data Sets and Ancillary Data	3
1.2 Correction and Calibration Strategies	3
2. Data Server Structure	5
3. File name convention	6
4. Contents of the Polarimetric File	7
5. Antenna Pattern File	14
6. Further reading	16
7. Disclaimer and Terms of Use	16
8. Data Citation	17
9. References	18
9.1 Papers on ROHP-PAZ mission and data	18
9.2 Other GNSS-PRO related studies	18

1. RO in PAZ: Brief Summary

The radio occultation (RO) experiment aboard the PAZ Low Earth Orbiter (LEO) is the first GNSS polarimetric RO mission (GNSS-PRO), designed to test the capability of polarimetric signatures in GNSS RO data to detect and quantify heavy rain and other hydrometeors [3].

The mission has been possible thanks to agreements between the Institute of Space Sciences (ICE-CSIC/IEEC, in charge of the experiment), Hisdesat (company that owns and exploits the PAZ satellite), NASA/JPL (scientific and payload support), NOAA (expansion of the ground segment for near-real time applications), and UCAR (low level data processing).

The hypothesis of the experiment is that the phase shift suffered by the horizontally polarized signals with respect to the vertically polarized ones carries information about heavy rain cells and other hydrometeors crossed along the ray. The hypothesis was confirmed in [1], where a simple processing and calibration approach was implemented. An improved calibration strategy was tested in [4], where residual systematic effects were also investigated. A thoughtful and theoretical insight into all the systematic effects can be found in [7].

The sets of data made public at ICE-CSIC/IEEC are **LEVEL-1b products**, i.e., **corrected and calibrated observables**. In particular, the observables are the carrier phase delay, in millimetres,

measured between the horizontally polarized component of the GNSS signal and the vertically polarized one ('polarimetric phase shift').

1.1 Lower Level Data Sets and Ancillary Data

The LEVEL-1a products used to generate these LEVEL-1b are **excess phase and SNR values pre-processed at UCAR**, in particular, from the 'conPhs' files of the UCAR GNSS RO suit. Metadata, and other steps of the processing have required information from UCAR LEVEL-2 files 'atmPrf', 'wetPrf' and platform information in 'leoAtt' files.

Some metadata in the polarimetric files have been obtained from Integrated MultisatellitE Retrievals for the Global Precipitation Measurement (GPM) mission (IMERG) (doi: 10.5067/GPM/IMERG/3B-HH/06) and from the NCEP/CPC L3 Half Hourly 4km Global merged Infrared brightness temperature (doi: 10.5067/P4HZB9N27EKU).

1.2 Correction and Calibration Strategies

ICE-CSIC/IEEC provides four types of polarimetric observables:

- **Original excess phase at each polarimetric port** (H/V), variables 'h_exL1' and 'v_exL1': these are copies of the same fields provided in UCAR's conPhs files, reproduced here for the users' convenience, with UCAR's permission.
- **Corrected polarimetric phase shifts**, variable 'dphase_corr': these are the results of subtracting the original V-polarized excess phase from the original H-polarized one, correcting any residual cycle slip, and setting an arbitrary zero at 30 km altitude.
- **Calibrated polarimetric phase shifts, linear fit model**, variable 'dphase_cal_lin': Removing the residual systematic effects (mostly instrumental, but also ionospheric) by a linear fit above 20 km altitude, and subtraction of the resulting trend. This is the approach used in [1].
- **Calibrated polarimetric phase shifts, antenna pattern**, variable 'dphase_cal_ant': Removing the residual systematic effects (mostly instrumental, but also ionospheric) by subtracting the antenna pattern. This is the approach used in [4], and the one giving lower noise levels in the rain-free set of profiles (RECOMMENDED). The antenna pattern is obtained in-orbit, as also explained in [4]. The antenna patterns used to calibrate the files are also available at this server (see Sections 2 and 5).

The plot in Figure 1-1 shows the basic processing steps involved to reach each calibrated observable. More details can be found in the references cited above.

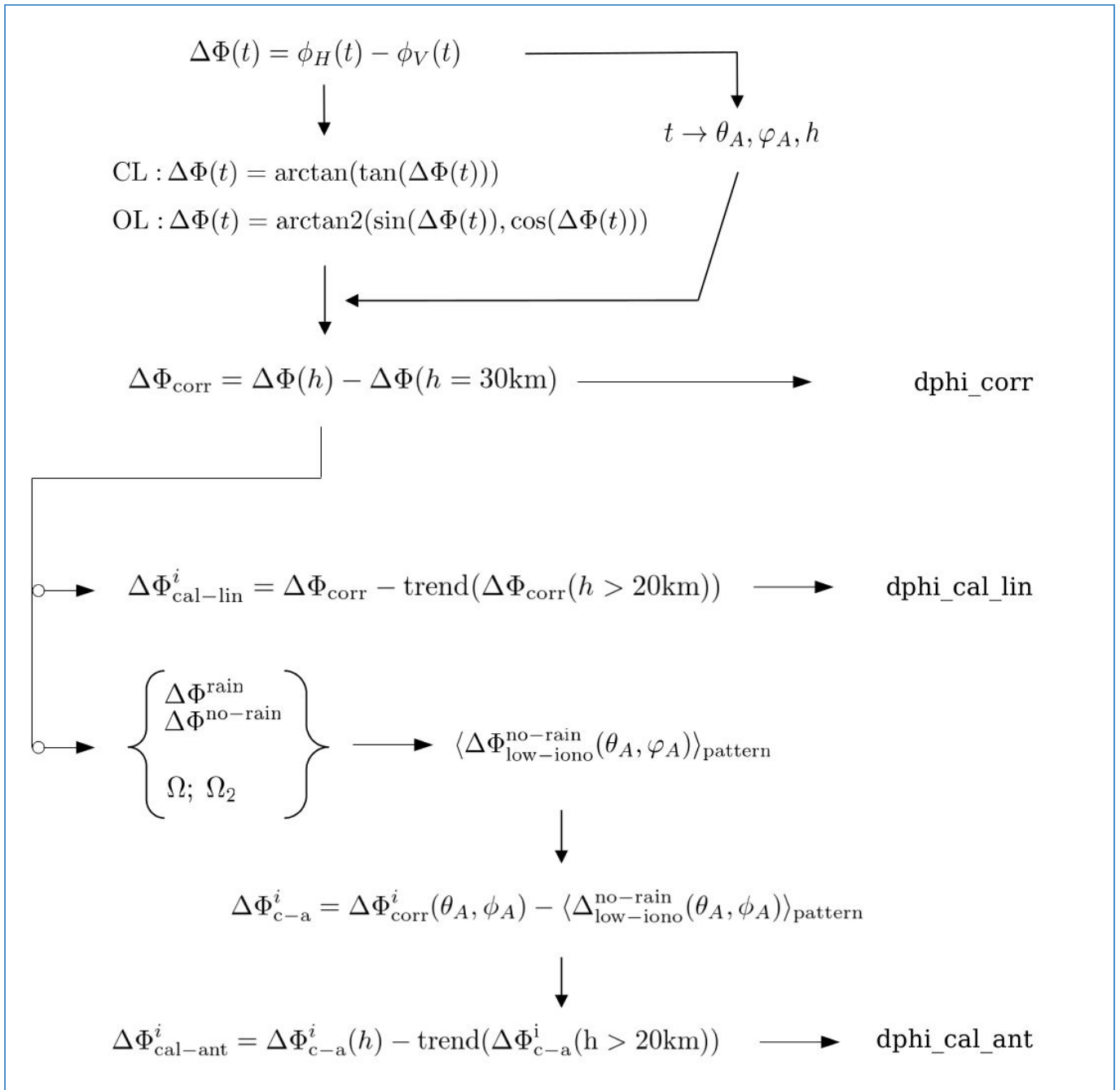


Figure 1-1: Steps in the processing of corrected and calibrated data. On the right side, the name of the relevant Level-1b variables in the netcdf file.

2. Data Server Structure

The polarimetric data can be downloaded at <https://paz.ice.csic.es/dataAcces.php?idi=EN>.

The datafiles are available for free, under a CC BY-NC license (see Section 7), after a quick registration step. The registration provides login-access information for you to download data whenever required.

Once you log-in, you will access the public directories, structured as follows (directories in **bold blue** characters, files in **red**):

First level:	mission (currently paz/).
Second level:	processing version ZZZZ.ZZZZ_V## (currently 2010.2640_V05/).
Third level:	data type (currently, level-1 polPhs/ and antenna pattern in-orbit calibration polAnt/ . Other data types will be added at this level, when available).
Fourth level:	For level-1 data, further subdirectories correspond to the years of data acquisition/observation, YYYY/ .

<https://paz.ice.csic.es/pub/>

paz/

```
|__ 2010.2640_V05/
|   |__ polPhs/
|   |   |__ YYYY/
|   |   |   |__ polPhs_PAZ1.YYYY.DOY_ZZZZ.ZZZZ_V##.tgz
|   |   |__ polAnt/
|   |   |   |__ polAnt_Pattern_YYYYMMDD.nc
```

Download notes

Example to download all PAZ polPhs files using wget (be aware that this may be a lot of data):

```
wget -rN -np -A.tgz --user=xxxx --ask-password https://paz.ice.csic.es/pub/paz/2010.2640_V05/polPhs
```

The individual files are packed in daily zipped tar files. Upon unpacking, the individual files are placed in a folder named after the date.



This work is licensed under a [Creative Commons Attribution-NonCommercial 4.0 International License](https://creativecommons.org/licenses/by-nc/4.0/).

3. File name convention

The GNSS polarimetric RO data obtained aboard PAZ and pre-processed to level-1b at ICE-CSIC/IEEC are based on level-1 data pre-processed at UCAR. To track back the UCAR level-1a files used at each profile, our file convention embeds UCAR's one:

polPhs_**UCAR-FILE-ID**_**UCAR-VER-ID**_v###.nc

Where the last number is the version of the processing code used at ICE-CSIC/IEEC for the correction and calibration of the polarimetric observables. The UCAR-FILE-ID includes: PAZ1 (LEO identifier), YYYY.DOOY.HH.MM. year, day of year, hour and minute of the RO event, GNN for the transmitter ID number, and the UCAR-VER-ID is a sequence ZZZZ.ZZZZ to identify the version of the processing software at UCAR:

polPhs_**PAZ1.YYYY.DOOY.HH.MM.GNN**_**ZZZZ.ZZZZ**_v###

The strings shown in red and green are inherited from the UCAR level-1a file, and can also be checked in the global attributes of the polarimetric file: **'filestamp_UCAR'** and **'version_UCAR'**, respectively.

4. Contents of the Polarimetric File

The files are in NETCDF4_CLASSIC, self-explanatory, format. A few more details are provided below.

DIMENSIONS:	
Dimension name:	Description:
time	Number of epoch-observations, at 50Hz rate
time_cal	Number of calibrated observation, interpolated at 50Hz rate
time_lr	Number of low resolution epochs for orbital information

VARIABLES WITH 'time' DIMENSION:		
Variable name:	Description:	Units:
time	Time of the 50 Hz data records, in seconds since start of occultation. The time since the start of occultation is given by the global attributes: 'year', 'doy', 'month', 'day', 'hour', 'minute' and 'second'.	s
h_exL1	Excess phase at the GPS L1 frequency and H-polarization, as provided in UCAR's conPhs files. The units, in millimeters of GPS L1 propagation, can be converted to radians as: $2 \pi h_exL1/\lambda_1$, where λ_1 is the wavelength of GPS L1 band carrier signal in mm ($\lambda_1 = 190.5$ mm).	mm
v_exL1	Excess phase of the GPS L1-frequency and V-polarization signal, as provided in UCAR's conPhs files. The units, in millimeters of GPS L1 propagation, can be converted to radians as: $2 \pi v_exL1/\lambda_1$, where λ_1 is the wavelength of GPS L1 band carrier signal in mm ($\lambda_1 = 190.5$ mm).	mm
h_caL1snr	Signal to noise ratio of the GPS L1-frequency, CA code, H-polarization signal, as provided in UCAR's conPhs files.	V/V
v_caL1snr	Signal to noise ratio of the GPS L1-frequency, CA code, V-polarization signal, as provided in UCAR's conPhs files.	V/V
height	Height above the mean sea level of the tangent point of each ray that corresponds to 50 Hz data. The tangent point is the point of the ray at lowest altitude. It has been considered with respect to a geoid with an undulation 'geoid_undulation' above an Earth of radius 'radiusOfCurvature' (see global attributes for descriptions of these values).	km

dphase_corr	Corrected differential polarimetric phase shift (H-V phases). The corrections include cycle slips and an arbitrary zero-anchoring at 30 km altitude. These polarimetric phase shifts are not calibrated, yet (see dphase_cal variables below for calibrated polarimetric shifts). The units, in millimeters of GPS L1 propagation, can be converted to radians as: $2\pi \text{ dphase_corr}/\lambda_1$, where λ_1 is the wavelength of GPS L1 band carrier signal in mm ($\lambda_1 = 190.5$ mm).	mm
--------------------	---------------------------------------------------------------------------------------------------------------------------------------------------------------------------------------------------------------------------------------------------------------------------------------------------------------------------------------------------------------------------------------------------------------------------------------------------------------------------------------------------------------	----

VARIABLES WITH 'time_cal' DIMENSION:

Variable name:	Description:	Units:
time_cal	Time corresponding to calibrated data, interpolated to 50 Hz. The time reference is given by the global attributes: 'year', 'doy', 'month', 'day', 'hour', 'minute' and 'second'. Calibration includes a 1 second smoothing of the data, therefore the resolution is effectively reduced.	s
height_cal	Height above the sea level of the tangent point of each ray that corresponds to 50 Hz <u>calibrated</u> data. The tangent point is the point of the ray at lowest altitude. It has been considered with respect to a geoid with an undulation 'geoid_undulation' above an Earth of radius 'radiusOfCurvature' (see global attributes for descriptions of these values). Calibration includes a 1 second smoothing of the data, therefore the resolution is effectively reduced.	km
dphase_cal_lin	Calibrated differential polarimetric phase shift (H-V) using linear trend . See doi:10.1029/2018GL080412 and doi:10.5194/amt-13-1299-2020 for details about this calibration method. The units, in millimeters of GPS L1 propagation, can be converted to radians as: $2\pi \text{ dphase_cal_lin}/\lambda_1$, where λ_1 is the wavelength of GPS L1 band carrier signal in mm ($\lambda_1 = 190.5$ mm).	mm
dphase_cal_ant	Calibrated differential polarimetric phase shift (H-V) using an antenna phase pattern . The antenna phase pattern identifier can be found in the global attribute 'ant_pattern_id', and the actual pattern file in the public server (see Section 2 of this document). This calibration methodology is explained in doi:10.5194/amt-13-1299-2020 . The units, in millimeters of GPS L1 propagation, can be converted to radians as: $2\pi \text{ dphase_cal_ant}/\lambda_1$, where λ_1 is the wavelength of GPS L1 band carrier signal in mm ($\lambda_1 = 190.5$ mm).	mm

VARIABLES WITH 'time_lr' DIMENSION:

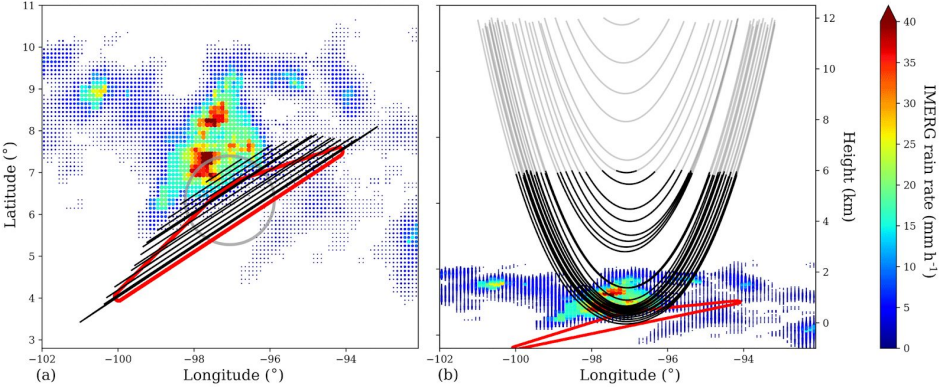
Variable name:	Description:	Units:
time_lr	Time for the lower resolution orbital data. The orbital variables are extracted from UCAR's conPhs files, but the time referenced to the time given in the global attributes: 'year', 'doy', 'month', 'day', 'hour', 'minute' and 'second'.	s
gps_x	GPS position: ECI coordinate X	km
gps_y	GPS position: ECI coordinate Y	km
gps_z	GPS position: ECI coordinate Z	km
gps_vx	GPS velocity: ECI coordinate X	km/s
gps_vy	GPS velocity: ECI coordinate Y	km/s
gps_vz	GPS velocity: ECI coordinate Z	km/s
leo_x	PAZ LEO position: ECI coordinate X	km
leo_y	PAZ LEO position: ECI coordinate Y	km
leo_z	PAZ LEO position: ECI coordinate Z	km
leo_vx	PAZ LEO velocity: ECI coordinate X	km/s
leo_vy	PAZ LEO velocity: ECI coordinate Y	km/s
leo_vz	PAZ LEO velocity: ECI coordinate Z	km/s

GLOBAL ATTRIBUTES:

Name:	Description:
filestamp_UCAR	Radio occultation identifier used in UCAR files.
lon	Longitude representative of the radio occultation event at the occultation point (as provided in UCAR's atmPrf files, defined when excess phase = 500 m). Bad values: -999.0: data not provided in the atmPrf (or missing atmPrf)
lat	Latitude representative of the radio occultation event at the occultation point (as provided in UCAR's atmPrf files, defined when excess phase = 500 m)

	Bad values: -999.0: data not provided in the atmPrf (or missing atmPrf)
prn	GPS transmitter identified linked to the pseudo random noise (PRN) code that transmits. The same code can be reused for another satellite once the former one is decommissioned.
svn	GPS transmitter satellite identification number. This number relates to each satellite (not the code transmitted).
az_surf	Azimuth of the radio occultation link, at the occultation point (as provided in UCAR's atmPrf files, defined when excess phase = 500 m). The angle is measured between North and the GPS direction of the raypath, positive to the East. Bad values: -999.0: data not provided in the atmPrf (or missing atmPrf)
year	Reference time for the dimensions 'time', 'time_cal' and 'time_lr'. It corresponds to the starting time of the profile: year
doy	Reference time for the dimensions 'time', 'time_cal' and 'time_lr'. It corresponds to the starting time of the profile: day of the year (doy)
month	Reference time for the dimensions 'time', 'time_cal' and 'time_lr'. It corresponds to the starting time of the profile: month
day	Reference time for the dimensions 'time', 'time_cal' and 'time_lr'. It corresponds to the starting time of the profile: day
hour	Reference time for the dimensions 'time', 'time_cal' and 'time_lr'. It corresponds to the starting time of the profile: hour
minute	Reference time for the dimensions 'time', 'time_cal' and 'time_lr'. It corresponds to the starting time of the profile: minute
second	Reference time for the dimensions 'time', 'time_cal' and 'time_lr'. It corresponds to the starting time of the profile: second (including fraction)
institution	File generated by the Institute of Space Sciences (ICE/CSIC) and the Institute for Space Studies of Catalonia (IEEC), Spain.
version_UCAR	Version of the UCAR processing software to generate the files used as input for this polarimetric processing.
version_ICE	Version of the ICE/CSIC/IEEC polarimetric processing software.
ant_pattern_id	Date reference that identifies the antenna pattern used to generate the calibrated differential phase shift. See Section 2 of this document to know where the antenna phase pattern file is found, and Section 5 for more information about the contents of this file.

radiusOfCurvature	Equivalent radius of curvature of the Earth, in km, when it is approximated as a sphere tangential to the Earth surface. It is estimated when excess phase = 500 m . This is used when estimating the heights of the rays' tangent points.
centerOfCurvature_offset	Vector in ECEF coordinates and km units, to be applied to the sphere of radius 'radiusOfCurvature', to be tangential at the surface of the Earth at the location of the radio occultation. This is used when estimating the heights of the rays' tangent points.
geoid_undulation	Undulation of the geoid with respect to the reference ellipsoid. This is used when estimating the heights of the rays' tangent points. Given in units of m.
t_CLOLtransition_h	Time in seconds since the start of the radio occultation, when the H-polarization channel of the receiver switches from phase lock look to open loop modes of operation.
t_CLOLtransition_v	Time in seconds since the start of the radio occultation, when the V-polarization channel of the receiver switches from phase lock look to open loop modes of operation.
meanPrecipitation_06	Surface rain rate in mm/h, obtained by co-location of the PAZ radio occultation profile with IMERG surface rain rate products. It corresponds to the IMERG average across a circle of diameter equivalent to 0.6° in the Equator. It is given in mm/h units. Precipitation values used in doi:10.1029/2018GL080412 . The IMERG file ID can be found in the attribute 'fname_IMERG'. Bad values: -1 : Precipitation processing failed. -999.0 : Location outside the range of precipitation mission coverage.
meanPrecipitation_2	Surface rain in mm/h, obtained by co-location of the PAZ radio occultation profile with IMERG surface rain products. It corresponds to the IMERG average across a circle of diameter equivalent to 2° in the Equator. It is given in mm/h units. Precipitation values used in doi:10.1029/2018GL080412 . The IMERG file ID can be found in the attribute 'fname_IMERG'. Bad values: -1 : Precipitation processing failed. -999.0 : Location outside the range of precipitation mission coverage.
meanPrecipitationBelow_6km	Surface rain in mm/h, obtained by co-location of the PAZ radio occultation profile with IMERG rain products. It corresponds to the IMERG average across the area of the rays below 6 km, projected onto the Earth surface. The co-location approach is detailed in doi:10.5194/amt-13-1299-2020 . See below Figure 3 of the paper, this rain value corresponds to the average inside the red line. It is given in mm/h units. The IMERG file ID can be found in the attribute

	<p>'fname_IMERG':</p>  <p>Bad values: -1 : No data from IMERG files -2 : Rays do not reach below 6 km. -999.0 : Location outside the range of precipitation mission coverage.</p>
<p>minBrightnessTemp_2</p>	<p>Minimum infrared brightness temperature found in NCEP CPC Tb products within a circle of diameter equivalent to 2° in the Equator. It is given in units of Kelvin. The NCEP file ID can be found in the attribute 'fname_NCEPCPC'.</p> <p>Bad values: -1 : No data from NCEP/CPC files (corrupted file or outside range of coverage)</p>
<p>cth_Tb</p>	<p>Approximate Cloud Top Height (CTH) estimated from the altitude of the PAZ radio occultation profile where the temperature (from UCAR's wetPrf file) corresponds to the attribute 'minBrightnessTemp_2'. In units of km.</p>
<p>freezingHeight</p>	<p>Altitude where the PAZ temperature profile (from UCAR's wetPrf file) is 0°C.</p> <p>Bad values: -1 : No data from wetPrf files or freezing height below minimum retrieved height</p>
<p>fname_IMERG</p>	<p>File name identifier for the IMERG product used to generate attributes 'meanPrecipitation_06', 'meanPrecipitation_2', and 'meanPrecipitationBelow_6km'.</p>
<p>fname_NCEPCPC</p>	<p>File name identifier for the NCEP CPC file used to generate the attributes 'minBrightnessTemp_2' and 'cth_Tb'.</p>
<p>dphi_0005</p>	<p>Average value, between surface and 5 km altitude, of the variable dphase_cal_ant, in this profile.</p> <p>Bad values (and equivalent for the following dphi values): -999.0: 'height_cal' variable does not reach below 5 km.</p>

dphi_0510	Average value, between 5 km and 10 km altitude, of the variable dphase_cal_ant, in this profile. Please check that height_flag is below this range of altitudes.
dphi_1015	Average value, between 10 km and 15 km altitude, of the variable dphase_cal_ant, in this profile. Please check that height_flag is below this range of altitudes.
dphi_0010	Average value, between surface and 10 km altitude, of the variable dphase_cal_ant, in this profile.
dphi_0015	Average value, between surface and 15 km altitude, of the variable dphase_cal_ant, in this profile.
dphi_max	Maximum value of the variable dphase_cal_ant, in this profile. Please check that it happens at an altitude above the warning height (dphi_max_h > height_flag).
dphi_max_h	Height that corresponds to the maximum value (dphi_max) of the variable dphase_cal_ant, in this profile. Please check that dphi_max_h > height_flag.
qc_conPhs	Quality flag provided in the UCAR's conPhs file. 1 = quality test passed, 0 = quality tests failed. UCAR's conPhs files are the input to generate the dphase variables here provided.
exists_atmPrf	Checks whether the UCAR's atmPrf file exists or not. 1 = file exists, 0 = file does not exist
qc_atmPrf	Quality flag provided in the UCAR's atmPrf file. 1 = quality test passed, 0 = quality tests failed.
exists_wetPrf	Checks whether the UCAR's wetPrf file exists or not. 1 = file exists, 0 = file does not exist
qc_wetPrf	Quality flag provided in the UCAR's wetPrf file. 1 = quality test passed, 0 = quality tests failed. UCAR's wetPrf files are here used to estimate 'cth_Tb' and 'freezingHeight' attributes.
height_flag	Warning about doubtful quality of the data below the indicated height. The user is advised to use caution when using data below the warning height, as the standard deviation of the data might be too large. This might indicate the signal track is momentarily lost, with unclear effects on polarimetric phase shift below that point.

5. Antenna Pattern File

The antenna pattern used to calibrate the polarimetric phase shift is kept in netcdf files. The pattern is generated with in-orbit data: PAZ profiles that correspond to rain-free conditions, and accumulated during long periods of time. The pattern can be updated from time to time, generating a new file with a distinctive filename, to identify the pattern used in the processing of each data file.

Please note that the antenna pattern file does NOT contain the gain/power/amplitude pattern, but a the H-V phase pattern (suitable for calibration of the polarimetric phase shift observables).

The filename convention is:

Antenna pattern filename convention:
polAnt_Pattern_YYYYMMDD.nc

Where YYYYMMDD is the date of creation of the antenna pattern. This date matches the value in the global attribute 'ant_pattern_id' of the 'polPhs' file.

It is given in the spherical coordinate system fixed to the satellite's body reference frame. The z axis points approximately towards the anti-velocity vector of the satellite and the x axis points approximately towards the center of the Earth. The y axis completes an orthogonal reference system. The vector from the PAZ antenna to the tracked GPS satellite is then described by an inclination angle (here defined as elevation), an azimuthal angle (here defined as azimuth) and its distance (not relevant here). Doing so we ensure a common reference frame for all occultations.

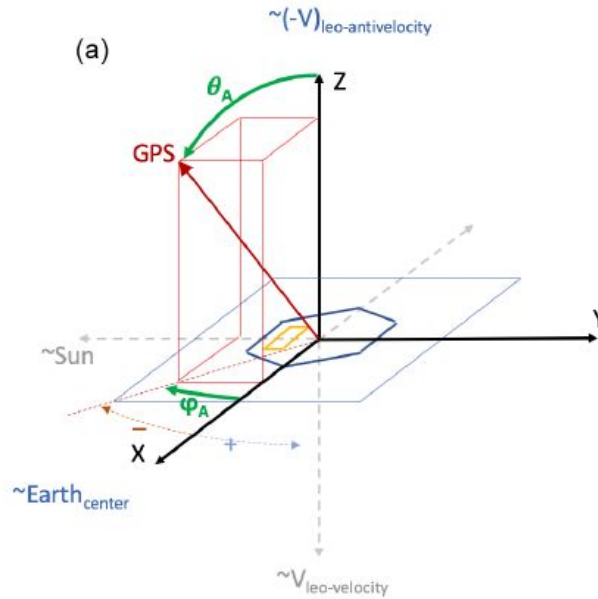


Figure 5-1: Antenna coordinate system used in the ice_antPattern files. Figure extracted from [4] (Figure 4-a in [4]).

The content of the file is:

DIMENSIONS:	
Dimension name:	Description:
azim	Number of bins for the gridded dimension azimuth
elev	Number of bins for the gridded dimension elevation

VARIABLES:	
Variable name:	Description:
azimuth	Angle φ_A as defined in Figure 5-1.
elevation	Angle θ_A as defined in Figure 5-1.
phase_pattern	Carrier phase difference between the H and V channels at each cell of the antenna pattern.

6. Further reading

Please visit <https://paz.ice.csic.es/> for news and other information related to the ROHP-PAZ mission.

OUTREACH MATERIALS:

<https://paz.ice.csic.es/outreach.php?idi=EN>

TECHNICAL DOCUMENTATION:

<https://paz.ice.csic.es/technicalDocumentation.php?idi=EN>

PEER-REVIEWED PAPERS, POSTERS PRESENTED TO CONFERENCES, ETC:

<https://paz.ice.csic.es/science.php?idi=EN>

7. Disclaimer and Terms of Use

The data and information in the data set provided here are intended for use by persons possessing technical skill and knowledge in remote sensing. While the data is provided in good faith and to the best of ICE-CSIC/IEEC knowledge, ICE-CSIC/IEEC does neither commit to it being updated nor warranties uninterrupted availability. Neither ICE-CSIC/IEEC nor any of its employees makes any warranty, express or implied, including warranties of fitness for a particular purpose, or assumes any legal liability or responsibility for the accuracy, completeness, or usefulness of any information provided.

While every effort is made to ensure the data quality, the data is provided “as is”. The burden of fitness of the data lies completely with the user. The accuracy of any user’s statistical analysis and any reported findings are not the responsibility of ICE-CSIC/IEEC. Nothing arising from the data should be taken to constitute ICE-CSIC/IEEC’s professional advice or a formal recommendation. ICE-CSIC/IEEC is not responsible for data management after extraction and transmission to the recipient.

ICE-CSIC/IEEC does not warrant that the files, the servers and the databases used for data storage, extraction, management and transmission are free of errors, viruses or bugs, and the recipient accepts that it is the recipient’s responsibility to make adequate provision for protection against such threats.

The data provided by the users during the registration process will not be shared with any third parties and they will be protected according to the European regulations.



This work is licensed under the Creative Commons Attribution-NonCommercial 4.0 International License. To view a copy of this license, visit <http://creativecommons.org/licenses/by-nc/4.0/> or send a letter to Creative Commons, PO Box 1866, Mountain View, CA 94042, USA.

8. Data Citation

If these data sets are used in publications, please cite the relevant references in Section 9.1, at least [1] or [3].

- For citations related to the mission and proof-of-concept demonstration, please cite [1] or [3];
- for validation studies, please cite [1] and [4];
- for calibration strategies, please cite [1] (linear) or [4] (antenna pattern);
- for description and studies on the systematic effects, please cite [7], [3] and/or [4]; and
- for the ground-based experimental campaign conducted before the spaceborne mission, please cite [6].

A suggested acknowledge sentence is:

“GNSS-PRO data acquired from the ROHP-PAZ mission aboard the PAZ satellite. The mission is a collaboration between ICE-CSIC/IEEC, Hidesat, NOAA, UCAR and NASA/JPL. Data available at <https://paz.ice.csic.es>, proof-of-concept study in doi:10.1029/2018GL080412, calibration strategy explained in doi:10.5194/amt-13-1299-2020.”

9. References

9.1 Papers on ROHP-PAZ mission and data

- [1] Cardellach, E., Oliveras, S., Rius, A., Tomás, S., C. O. Ao G. W. Franklin B. A. Iijima D. Kuang T. K. Meehan R. Padullés M. de la Torre Juárez F. J. Turk D. C. Hunt W. S. Schreiner S. V. Sokolovskiy T. Van Hove J. P. Weiss Y. Yoon Z. Zeng J. Clapp W. Xi-Serafino F. Cerezo, Sensing heavy precipitation with GNSS polarimetric radio occultations, *Geophysical Research Letters*, 46, 2, pp. 1024-1031, 2019, jan, [doi:10.1029/2018GL080412](https://doi.org/10.1029/2018GL080412)
- [2] Cardellach, E., Padullés, R., Tomás, S., Turk, F. J., Ao, C. O. and de la Torre-Juárez, M., Probability of intense precipitation from polarimetric GNSS radio occultation observations. *Q.J.R. Meteorol. Soc.*, 2017, [doi:10.1002/qj.3161](https://doi.org/10.1002/qj.3161)
- [3] Cardellach, E., Tomas, S., Oliveras, S., Padullés, R., Rius, A., De la Torre-Juárez, M., Turk, F.J., Ao, C.O., Kursinski, E.R., Schreiner, B., Ector, D., Cucurull, Sensitivity of PAZ LEO Polarimetric GNSS Radio-Occultation Experiment to Precipitation Events, *IEEE Transactions on Geoscience and Remote Sensing*, 2014, 53(1), [doi:10.1109/TGRS.2014.2320309](https://doi.org/10.1109/TGRS.2014.2320309)
- [4] Padullés, R., Ao, C. O., Turk, F. J., de la Torre Juárez, M., Iijima, B., Wang, K. N., and Cardellach, E., Calibration and validation of the Polarimetric Radio Occultation and Heavy Precipitation experiment aboard the PAZ satellite, *Atmos. Meas. Tech.*, 13, 1299–1313, 2020, [doi:10.5194/amt-13-1299-2020](https://doi.org/10.5194/amt-13-1299-2020)
- [5] Padullés, R., Cardellach, E., Rius, A., Untangling rain structure from polarimetric GNSS Radio Occultation observables: a 2D tomographic approach, *European Journal of Remote Sensing*, 49, pp. 571-585, 2016, [doi:10.5721/EuJRS20164930](https://doi.org/10.5721/EuJRS20164930)
- [6] Padullés, R., Cardellach, E., de la Torre Juárez, M., Tomás, S., Turk, F. J., Oliveras, S., Ao, C. O., and Rius, A.: Atmospheric polarimetric effects on GNSS Radio Occultations: the ROHP-PAZ field campaign, *Atmos. Chem. Phys.*, 16, 635-649, 2016, , [doi:10.5194/acp-16-635-2016](https://doi.org/10.5194/acp-16-635-2016)
- [7] Tomás, S., Padulles, R., Cardellach, E., Separability of Systematic Effects in Polarimetric GNSS Radio Occultations for Precipitation Sensing, *IEEE Transactions on Geoscience and Remote Sensing*, 56, 8, pp. 4633-4649, 2018, [doi:10.1109/TGRS.2018.2831600](https://doi.org/10.1109/TGRS.2018.2831600)

9.2 Other GNSS-PRO related studies

- A. Turk, J. F., Padullés, R., Ao, C. O., de la Juárez, M. T., Wang, K., Franklin, G. W., Lowe, S. T., Hristova-Veleva, S. M., Fetzer, E. J., Cardellach, E., et al, Benefits of a Closely-Spaced Satellite Constellation of Atmospheric Polarimetric Radio Occultation Measurements, *Remote Sensing*, 11, 20, 2019, [doi:10.3390/rs11202399](https://doi.org/10.3390/rs11202399)
- B. [Bonafoni, S., Biondi, R., Brenot, H., Anthes, R., Radio occultation and ground-based GNSS products for observing, understanding and predicting extreme events: A review, *Atmospheric Research* 230 \(104624\), 2019, doi:10.1016/j.atmosres.2019.104624](https://doi.org/10.1016/j.atmosres.2019.104624)

- C. Murphy, M. J., Haase, J. S., Padullés, R., Chen, S.-H., Morris, M. A., The potential for discriminating microphysical processes in numerical weather forecasts using airborne polarimetric radio occultations, Remote Sensing, 11, (19), pp. 1-25, 2019, doi: 10.3390/rs11192268
- D. An, H., Yan, W., Bian, S., Ma, S., Rain monitoring with polarimetric GNSS signals: Ground-based experimental research, Remote Sensing, 11, (19), pp 1-19, 2019, doi: 10.3390/rs11192293
- E. Padullés, R., Cardellach, E., Wang, K.-N., Ao, C. O., Turk, F. J., de la Torre Juárez, M., Assessment of global navigation satellite system (GNSS) radio occultation refractivity under heavy precipitation, Atmospheric Chemistry and Physics, 18, pp. 11697-11708, 2018, doi: 10.5194/acp-18-11697-2018
- F. An, H., Yan, W., Huang, Y., Ai, W., Wang, Y., Zhao, X., Huang, X., GNSS Measurement of Rain Rate by Polarimetric Phase Shift: Theoretical Analysis, Atmosphere, 7, (8), pp 101, 1-12, 2016, doi:10.3390/atmos7080101
- G. An, H., Yan, W., Huang, Y., Zhao, X., Wang, Y., Ai, W., Feasibility Study of Rain Rate Monitoring from Polarimetric GNSS Propagation Parameters, Atmosphere, 7, (12), pp 159, 1-12, 2016, doi:10.3390/atmos7120159